

**An Purposive Vision Approach to Concrete Crack Inspection  
- Automated Registration and Crack Measurement in Multi-resolution Image Acquisition -**

**Takeshi DOIHARA, Kazuo ODA, Tsuyoshi KONDO, Masayoshi OBATA, Yoshizumi YASUDA\* (Japan)**

Research Institute, Asia Air Survey Co., Ltd.  
8-10 Tamura-cho, Atsugi-shi, Kanagawa, 243-0016  
Email: ta.doihara@ari.ajiko.co.jp, kz.oda@ari.ajiko.co.jp, ts.kondo@ari.ajiko.co.jp, ms.obata@ari.ajiko.co.jp  
JAPAN

\*Professor, Dept. of Information and Computer Sciences, Chiba Univ.  
Yayoi-cho, Inage-ku, Chiba-shi, Chiba, 263-0022  
Email: yasuda@icsd5.tj.chiba-u.ac.jp  
JAPAN

Commission V, Working Group V/III

**KEY WORDS:** Crack Measurement, Image Registration, Mosaic, Hierarchical Image Processing, Levenberg-Marquardt Method.

**ABSTRACT**

This paper discusses utilization of automatic 2-D image registration technique for efficient image data acquisition for concrete crack inspection. The proposed concept consists of multi-resolution image acquisition and image registration in which high-resolution images of high-precision are registered and placed upon a low-resolution image. The low-resolution image can show entire aspect of object to inspect and also can identify portions of the high resolution images which can be used for precise crack measurement. Registration procedure is based upon local projective transformation in which parameters of 2-D transformation are determined by enhanced Levenberg-Marquardt (LM) algorithm. Experimental results have concluded that multi-scale images can be registered by 2-D image mosaicing algorithm with image enhancement.

**1. INTRODUCTION**

Periodical crack inspection of concrete structure involves measurement of crack width by using crack-scale manually and/or by using digital image processing with close range photographs. Precise measurement by digital image processing technique requires large-scale photographs. For example, if crack-width must be measured in very high precision such as 0.1 mm, digital images should be captured with resolution of 0.025mm/pixel (Doihara et al., 1992). However, there is a trade-off between image resolution and amount of image data: 20000 x 20000 pixel<sup>2</sup> of image is required to cover 50cm x 50 cm area with the above resolution. If larger area have to be captured with the same resolution, the amount of image data will explode.

This paper proposes an purposive vision approach to concrete crack inspection with multi-resolution image acquisition strategy which offers solution for this trade-off. Multi-resolution image acquisition strategy consists of multi-resolution image capturing and image registration procedure in which high-resolution images of high-precision are registered and placed upon a low-resolution image (Figure 1). The low-resolution image can show entire aspect of

objects to inspect and also can identify positions of the high resolution images which can be used for precise crack measurement.

Images can be registered by 2-D projective transformation whose parameters are computed by Levenberg-Marquardt (LM) algorithm. Ordinary LM calculation often fails to register images with little textures such as fresh concrete, therefore the calculation is preceded by image enhancement.

This paper mainly discusses the 2-D image registration method with image enhancement which is one of the basic techniques to realize multi-resolution image acquisition strategy. This technique does not require any special target to be pasted or measured but merely demands rough measurement of corresponding points between the images to be registered. In this paper the theory of 2-D mosaicing with LM method is reviewed and its modification with image enhancement is introduced. Finally, results of image registration for various scales of images will be reported and discussed.

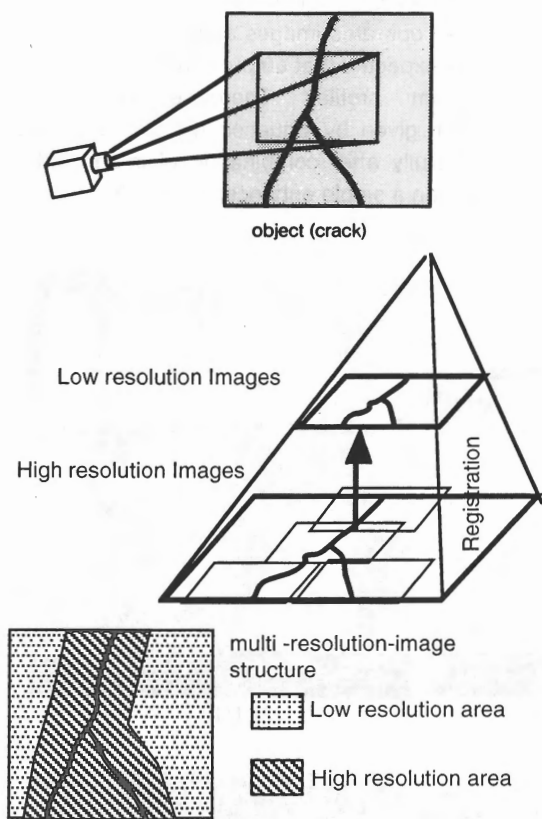


Figure 1: A Schema of multi-resolution image acquisition strategy

## 2. THEORY OF IMAGE REGISTRATION

### 2.1 Image registration with 2-D image mosaicing Method

The algorithm of image registration adopted here is based on 2-D image mosaicing method which can automatically match one image with another. This algorithm assumes that correspondence of coordinates between two images  $I$  and  $I'$  is registered by projective transformation:

$$\begin{aligned} x'(x, y, H) &= \frac{h_1x + h_2y + h_3}{h_7x + h_8y + 1} \\ y'(x, y, H) &= \frac{h_4x + h_5y + h_6}{h_7x + h_8y + 1} \end{aligned} \quad (1)$$

where  $(x, y)$  and  $(x', y')$  are coordinates of Image  $I$  and  $I'$ , and  $H(h_1, \dots, h_8)$  is a set of coefficients of projective transformation. In many cases 2-D image mosaicing adopts Levenberg-Marquardt (LM) algorithm to calculate  $H(h_1, \dots, h_8)$  automatically (Szeliski, 1994). The LM algorithm is a non-linear optimization which is an extension of

least square minimization (Press et al., 1992). Here LM algorithm optimizes  $H(h_1, \dots, h_8)$  which minimize the following evaluation function  $\chi^2(H)$ :

$$\begin{aligned} \chi^2(H) &= \sum_{i=1}^N e_i^2 \\ e_i &= I(x_i, y_i) - I'(x'(x_i, y_i, H), y'(x_i, y_i, H)) \end{aligned} \quad (2)$$

where  $I(x, y)$  and  $I'(x', y')$  are pixel value of image  $I$  and  $I'$ .

Many cases of 2-D image mosaicing employs coarse-to-fine strategy which refines precision by processing series of images structured hierarchically in different scales from coarse to fine. This strategy contributes to avoiding converge at local minimum of  $\chi^2(H)$ , as well as reduces processing time.

LM method requires initial estimation of  $H(h_1, \dots, h_8)$ . Since in most cases  $H(h_1, \dots, h_8)$  can be approximately regarded as Helmart transformation which contains transision, rotation and scaling, rough measurement of coordinates of two corresponding points gives good estimation of  $H$  by solving Equation (1) with these coordinates under following conditions:

$$\begin{aligned} h_1 &= h_5 \\ h_2 &= -h_4 \\ h_7 &= 0 \\ h_8 &= 0 \end{aligned} \quad (3)$$

### 2.2 2-D Image registration with image enhancement

Registration of images with little textures often fails to converge because  $\chi^2(H)$  does not have sharp peak at the minimum. The difference of optical conditions between two images, such as lighting condition or optical condition of cameras and lenses, also causes failure of computation because Equation (2) assumes that corresponding pixels of the image  $I$  and  $I'$  have the same value. These problems can be fatal to image registration that show concrete surface with less textures except cracks, and/or with various scales (or various focal lengths).

These problems can be solved by performing some proper enhancement on the images. Such a kind of image enhancement includes:

- Histogram equalization
- Laplacian filter
- Combination of Histogram equalization and Laplacian filter

Histogram equalization expands a range of distribution of pixel value so that textures on the images are exagger-

ated. Moreover, histogram equalization forces images to share identical histogram profile so that corresponding pixels have almost same value between the images. Note that the histograms before equalization should be counted within the area where two images overlap.

Laplacian filter does not equalize histogram profile of images at all, but it can normalize pixel values on edges to

0. And Laplacian filter also approximately works as band-pass filter and removes low frequency noise effectively. If Laplacian filter operates images after histogram equalization, it can be expected that output images also have identical histogram profiles. Therefore the evaluation function  $\chi^2(H)$  given by Equation (2) can be computed more successfully after combination of image enhancement rather than a single enhancement itself.

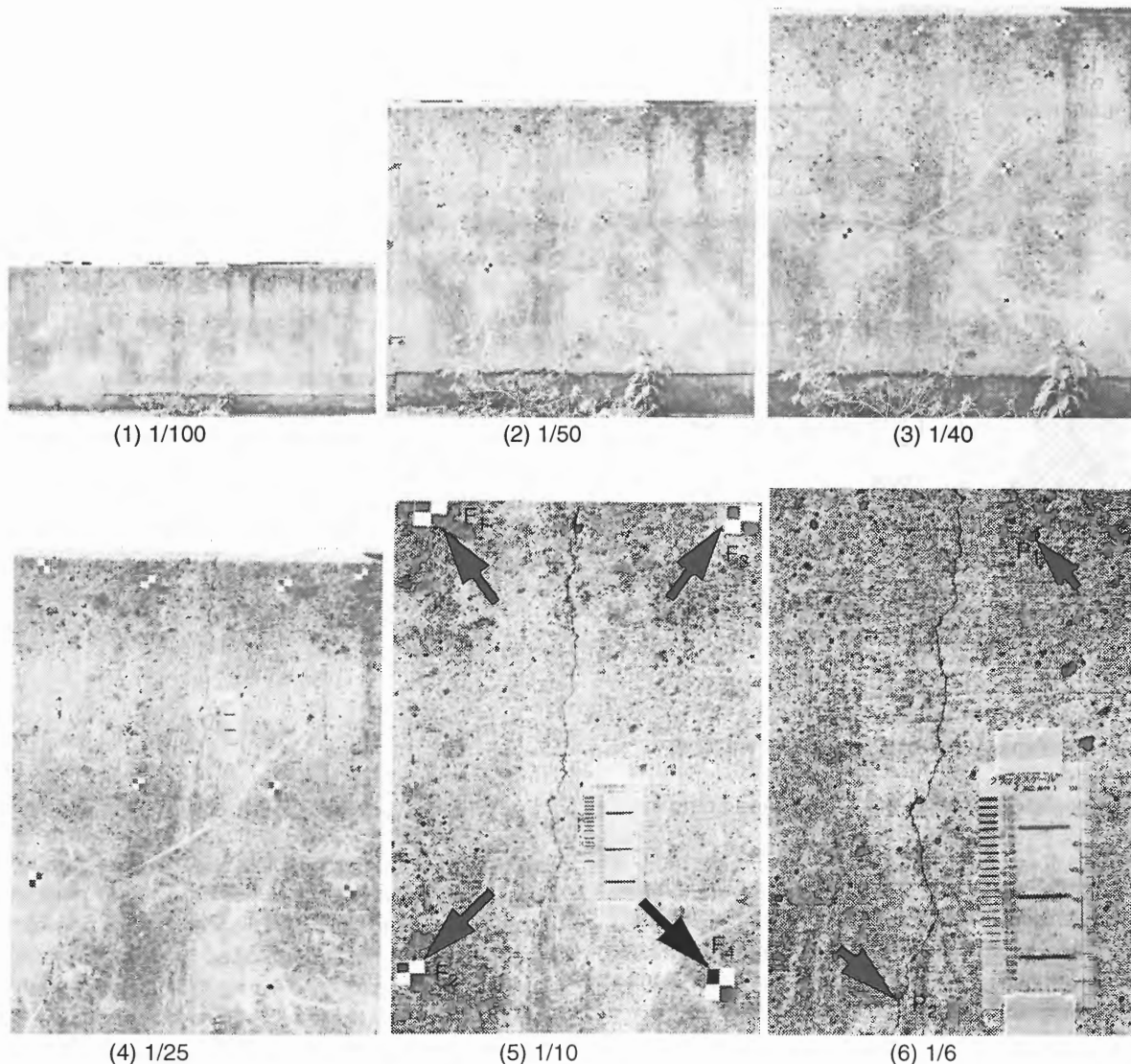


**Figure 2: The test images of various scales**

P<sub>1</sub> - P<sub>2</sub>: Feature points measured for initial estimation  
 F<sub>1</sub> - F<sub>4</sub>: Targets measured for checking precision of registration

### 3. EXPERIMENT AND RESULT

#### 3.1 Procedure of experiment

An experiment of registering multi-scale images of a concrete wall was undertaken to prove the effect of image enhancement.

Six test images (1) - (6) of a concrete wall were captured by a 35mm camera with various scales ranging from 1/100 to 1/6 (see Figure 2). A film scanner converted these images to digital format at the resolution of 2700 dpi. Fifteen pairs of these images are registered by a 2-D image mosaicing program.

The image registration test consists of the following steps (see in Figure 3).

- Measurement of coordinates of feature points and targets**  
 An operator manually measures coordinates of the feature points  $P_1$ -  $P_2$  (shown in Figure 2 (6)) and the targets  $F_1$ - $F_4$  (shown in Figure 2 (5)) in each image to be registered. The coordinates of  $P_1$ -  $P_2$  are used for initial estimation of projective transformation parameters and the coordinates of  $F_1$ - $F_4$  for calculation of precision. The test image (6) does not have the targets  $F_1$ - $F_4$ , thus the coordinates of the targets of this image can be estimated from the coordinates of the targets in the test image (5) and computed projective transformation between the test image (5) and (6).

- Image enhancement**  
 Preparing three types of image enhancement (histogram equalization (type 1), Laplacian filter (type 2), and combination of histogram equalization and Laplacian filter (type 3)), each type of enhancement was performed on every image.
- Image Registration**  
 The pair of enhanced images are registered by 2-D image mosaicing algorithm. Initial estimation of projective transformation is calculated by solving Equation (1) and (3) with the coordinates of  $P_1$  and  $P_2$  (see 2.1).
- Production of a multi-resolution image**  
 The pair of images are merged into a multi-resolution image according to calculated projective transformation  $H$  (see Figure 4).
- Calculation of Precision**  
 Precision of image registration  $E(H)$  are defined as the mean value of residual error at the targets  $F_1 - F_4$ , that is:

$$E(H) = \frac{\sum_{i=1}^4 D(F_{Si}, F'_{Si}(H, F_{Li}))}{4} \quad (4)$$

where  $F_{Si}$  is the measured coordinates of the target  $F_i$  in the smaller-scale image,  $F_{Li}$  the measured coordinates of the target  $F_i$  in the larger-scale image,  $F'_{Si}$  the estimated coordinates of  $F_i$  in the smaller-scale image by  $H$  and  $F_{Li}$ , and  $D(F_{Si}, F'_{Si})$  the distance between coordinates  $F_{Si}$  and  $F'_{Si}$ .

The results of registration are judged as converged correctly when the precision is less than 2 pixels except for the cases around the test image (6). The estimated coordinates of the targets  $F_1$ - $F_4$  are used in these cases because no target can be taken in the image (6).

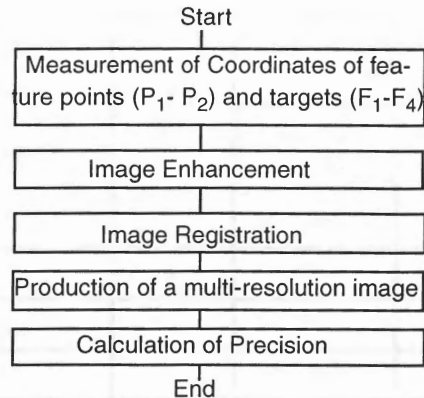


Figure 3: The flow chart of the image registration test

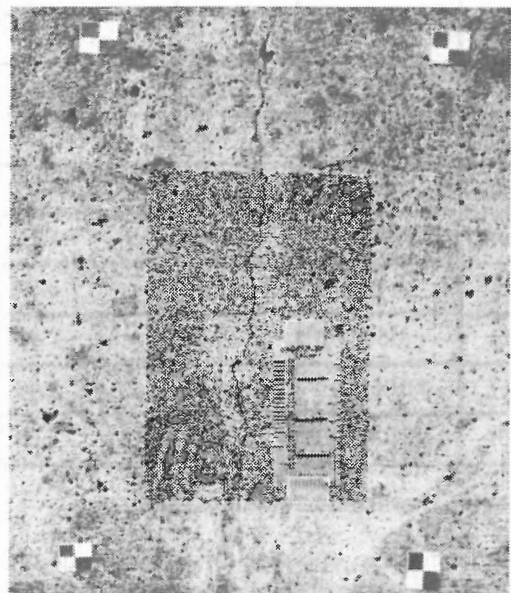


Figure 4: A multi-resolution image (the test image (4) and (6))

### 3.2 Effectivity of image enhancement

Table 1 shows the result of the image registration test. The first two columns shows the registered image pairs. Next column, which is the sort key of this table, shows the relative scale between the image pairs. Precision of the registration with or without image enhancement are shown in the other columns together with precision of initial estimation. Hatched cells indicates failing in calculation.

The table shows that image enhancement worked effectively in registration between image pairs whose relative scales are large. Image pairs with relative scale larger than 5 does not converge correctly without image enhancement. Among three types of image enhancement, type 1 (histogram equalization) and type 3 (combination of histogram equalization and Laplacian filter) works better than type 2 (Laplacian filter). Note that precisions of image registration are improved from those of initial estimation over every pair.

**Table 1: Result of registration between images of different scales**

| Registered image pairs |                | Relative Scale | Precision of initial estimation (pixel) | Precision (pixel) (Hatched cell: Not converged correctly) |                        |                    |                          |
|------------------------|----------------|----------------|---|---|------------------------|--------------------|--------------------------|
| Image No.              | Original Scale |                |   | No Enhancement  | Histogram Eq. (type 1) | Laplacian (type 2) | Hist.Eq. & Lap. (type 3) |
| (2)-(3)                | 1/50-1/40      | 1.2            | 2.19                                    | 0.56  | 0.57                   | 0.56               | 0.67                     |
| (3)-(4)                | 1/40-1/25      | 1.6            | 2.14                                    | 0.61  | 0.67                   | 0.64               | 0.78                     |
| (5)-(6)                | 1/10- 1/6      | 1.7            | 25.98                                   | 1.51  | 0.59                   | 0.76               | 0.70                     |
| (1)-(2)                | 1/100-1/50     | 2.0            | 2.10                                    | 0.68  | 0.50                   | 0.98               | 0.94                     |
| (2)-(4)                | 1/50-1/25      | 2.0            | 2.10                                    | 0.73  | 0.79                   | 1.09               | 0.95                     |
| (1)-(3)                | 1/100-1/40     | 2.5            | 6.84                                    | 1.30  | 1.37                   | 1.09               | 0.87                     |
| (4)-(5)                | 1/25-1/10      | 2.5            | 6.84                                    | 1.41  | 1.45                   | 1.07               | 1.04                     |
| (1)-(4)                | 1/100-1/25     | 4.0            | 3.25                                    | 1.01  | 0.99                   | 0.91               | 0.60                     |
| (3)-(5)                | 1/40-1/10      | 4.0            | 3.25                                    | 0.90  | 1.05                   | 0.89               | 0.97                     |
| (4)-(6)                | 1/25- 1/6      | 4.2            | 13.91                                   | 5.31  | 5.73                   | 5.31               | 5.90                     |
| (2)-(5)                | 1/50-1/10      | 5.0            | 4.21                                    | 0.86  | 0.69                   | 0.92               | 0.75                     |
| (3)-(6)                | 1/40- 1/6      | 6.7            | 8.82                                    | 1412.23   | 2.01                   | 2.78               | 2.89                     |
| (2)-(6)                | 1/50- 1/6      | 8.3            | 7.43                                    | 5428.47   | 2.20                   | 2.99               | 2.49                     |
| (1)-(5)                | 1/100-1/10     | 10.0           | 2.40                                    | 50.81   | 1.05                   | 1.07               | 1.10                     |
| (1)-(6)                | 1/100- 1/6     | 16.7           | 3.56                                    | 467.38  | 2.56                   | 19.30              | 4.41                     |

**3.3 Required precision for initial estimation**

As described above, one of the merits of image registration is that initial estimation of projective transformation is improved through automatic optimization. This means that image registration bears some sort of error in initial estimation.

To investigate how large errors are allowed in initial estimation, a series of image registration were executed with simulated errors. Positions of P<sub>1</sub> and P<sub>2</sub> are arranged to involve error vector  $\vec{r}_1$  and  $\vec{r}_2$ , whose direction and length were determined at random (see Figure 5). These errors were simulated in the lower-scale image in which the effect of error can be more serious.

Using type 1 enhancement, four hundred cases were tested in registration between the test image (1) and (5), whose relative scale is 10. Each results of registration were verified with a threshold of 2 pixel in precision. All cases were plotted in a 2-D graph with regard to relative error R<sub>1</sub> and R<sub>2</sub> whose definition is:

$$R_1 = \frac{|\vec{r}_1|}{D}$$

$$R_2 = \frac{|\vec{r}_2|}{D} \tag{5}$$

where D is the distance between P<sub>1</sub> and P<sub>2</sub>.

Figure 6 shows result of the test. The correct cases are indicated by small dots, while incorrect cases are indicated by triangles. The result shows that most of registration were converged correctly when R<sub>1</sub><0.15 and R<sub>2</sub><0.15, concluding that this image registration method allows 15% relative error in measurement of two features P<sub>1</sub> and P<sub>2</sub> for initial estimation. In test data (1), D is about 160 pixels and thus the initial estimation allows very rough measurement of feature points with error up to 24 pixels.

**4. CONCLUSION**

The multi-scale image acquisition strategy with multi-scale image registration is proposed. From the result of experiments, it is concluded that multi-scale image registration of concrete cracks can be achieved by automatic computa-

tion in spite of roughly initial estimation. And it can be emphasized that an purposive vision approach which adopts the multi-resolution image acquisition strategy offers solution for the trade-off between precise measurement and image data explosion.

### 5. REFERENCES

Doihara, T., et al., 1998. Hierarchical image processing for crack measuring on concrete structures. J. of the Japan Society of Photogrammetry and Remote Sensing (printing).

Press, W.H., et al., 1992. Numerical recipes in C: the art of scientific computing. Cambridge University Press, Cambridge, England, Second Editing.

Szeliski, R., 1994. Image Mosaicing for Tele-Reality Applications. DEC CRL 94/1.

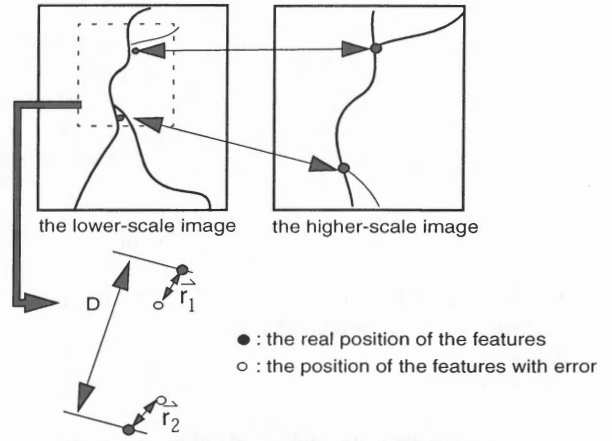


Figure 5: Measurement of coordinates of the feature points with error

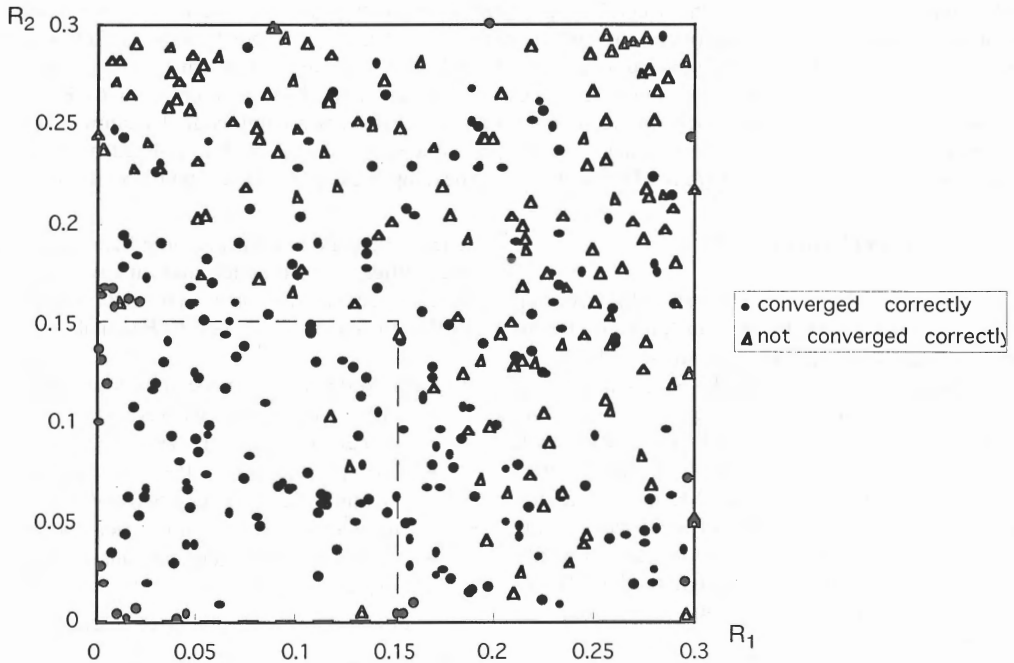


Figure 6: The result of the simulation test with errors in initial estimation